Micromachines **2013**, *4*, 286-305; doi:10.3390/mi4030286

OPEN ACCESS

micromachines

ISSN 2072-666X

www.mdpi.com/journal/micromachines

Article

Approaches for a Fair Comparison and Benchmarking of Electromagnetic Vibration Energy Harvesters

Clemens Cepnik and Ulrike Wallrabe *

Laboratory of Micro Actuators, University of Freiburg, IMTEK, Georges-Köhler-Allee 102, 79110 Freiburg, Germany; E-Mail: Clemens.Cepnik@imtek.de

* Author to whom correspondence should be addressed; E-Mail: wallrabe@imtek.uni-freiburg.de; Tel.: +49-761-203-7580; Fax: +49-761-203-7439.

Received: 16 May 2013; in revised form: 24 June 2013 / Accepted: 25 June 2013 / Published: 5 July 2013

Abstract: The performance of more than 60 different electromagnetic energy harvesters described in more than 100 publications is benchmarked. The benchmarking is based on earlier published parameters from literature as well as on two novel parameters introduced in this paper. The former allow to compare different harvester conversion principles as well as harvesters of different electrodynamic design principles. The latter consider the impact of ambient and boundary conditions for the most important sub-group, namely the resonant electrodynamic harvesters. The special consideration of how the mechanical damping and the energy conversion effectiveness depend on these conditions enables a fairer benchmarking of this common harvester type. High performing prototypes are identified, and the key parameters are provided for explanation. Finally, beneficial design approaches and the main challenges to maximize the output power are pointed out.

Keywords: review; benchmarking; figure of merit; comparison; optimization; electrodynamic energy harvesting; electromagnetic linear generators; power MEMS

---

1. Introduction

In our very recently published review paper [1] we provided an overview on electrodynamic vibration harvesters that have been published in the past 15 years. We discussed the different designs with different shapes and dimensions and pointed out the huge range of output powers across six orders of magnitude

from nW to mW. They were measured at similar, but also at quite different excitation accelerations and frequencies. The diversity of prototypes and output powers raises the question of how harvesters can fairly be compared. An answer would allow to identify the best design approaches and, if existing, the optimum harvester design without adapting each harvester concept to the same boundary conditions.

As the power density does not consider the excitation of a harvester, several authors reviewed and compared electrodynamic vibration harvesters based on different benchmarking parameters. Mitcheson [2] introduced a parameter to compare the harvester power to a theoretical power limit. However, this approach did not consider the scaling of the electrodynamic principle. Arnold used the power density per squared excitation acceleration [3] to account for the increasing power at stronger excitations. Based on the linear harvester model, Stephens [4] argued that this benchmarking parameter did not correctly consider the impact of the volume. None of the benchmarking approaches, however, could satisfiably explain the huge differences in the output power of published harvesters ranging from nW to mW.

In this paper we address the challenge to consider the complex impact of ambient and boundary conditions in a single benchmarking parameter. By considering the dependencies of key parameters such as the mechanical damping, an attempt to approach a fair benchmarking is provided. First, the benchmark parameters (BPs) from literature are briefly reviewed. Second, we introduce two novel parameters derived from the linear resonant harvester model. Third, based on the different BPs, the harvesters from our review paper [1] are benchmarked. The results allow to identify high performing harvester designs and design elements and to finally point out beneficial design rules.

2. Benchmarking Parameters for Different Harvesting Mechanisms

To compare different harvesting mechanisms among each other or harvesters to energy sources such as batteries, the power density, subsequently named BP (a), is often used.

$$BP_{(a)} = \frac{P_{avg}}{V} \tag{1}$$

P_{avg} is the measured average power a harvester can generate and V is its total volume. The power density just tells within which period of time a certain harvester at a particular excitation can provide the same energy as a battery of the same volume.

Mitcheson *et al.* [2,5,6] introduced a bottom-up approach to benchmark vibration harvesters with different harvesting principles against a theoretical limit. The assumption they made was that the harvester volume is completely used for the linear oscillator as well as the oscillator displacement, and additional volumes, e.g., for coil, housing, air gaps *etc.*, were neglected. Furthermore, the mechanical damping was neglected and the oscillator was only damped electrically without any energy dissipation in the mechanics or in the coil. The theoretical limit of the average power $P = \int m\ddot{x}\, d\dot{x}$ with x sinusoidal in the frequency domain is given by

$$P_{limit} = \frac{1}{2} m \hat{A}_{\perp} \omega_0 \hat{X}_{\perp} \tag{2}$$

where m is the oscillator mass and $\hat{X}_{\perp}$ its displacement amplitude, $\hat{A}_{\perp}$ is the excitation acceleration amplitude and ω_0 the eigenfrequency (Equation (3) differs from [2,5–7] by a constant factor as a mistake

in the derivation was corrected). With m expressed by the harvester volume minus the volume that is penetrated above and underneath the vibrating oscillator, one can find the optimum relation $\hat{X}_\perp = h/4$ between the harvester height h and the oscillator displacement amplitude $\hat{X}_\perp$ by differentiating with respect to h ($\hat{X}_\perp$ points into the direction of h).

$$P_{limit} = \frac{1}{8}\rho_m V h \omega_0 \hat{A}_\perp \tag{3}$$

and dividing the measured harvester power P_{avg} by this theoretical maximum leads to BP (b).

$$BP_{(b)} = \frac{P_{avg}}{\frac{1}{8}\omega_0 \rho_m V h \hat{A}_\perp} \tag{4}$$

BP (b) allows to compare any vibration harvesting principle at sinusoidal excitation (Note: The requirement is a sinusoidal excitation force. A harvester that converts energy nonlinearly but is harmonically excited can convert much more power due to the nonlinear forces.) with a theoretical (not approachable) limit. In fact, BP (b) is much smaller than unity, because the mechanical damping usually is at the level of the electrical damping. Additionally, the practical oscillator amplitude often is small compared with the harvester height h. Therefore, BP (b) prefers harvesters with a small height and eigenfrequency providing a realistic chance to approach $h/4$ with the oscillator amplitude.

3. Benchmarking of Resonant Electrodynamic Harvesters

Comparing only resonant electrodynamic harvesters allows to consider the impact of ambient and boundary conditions. A first benchmarking approach was derived from the linear harvester model by Arnold *et al*. [3] and shall be expanded here. The discussion is based on the fundamental equation we derived in [8]

$$P_{avg} = \frac{V_c k_c B_\perp^2}{V_c k_c B_\perp^2 + \rho_c d_m} \cdot \frac{(\rho_m V_m)^2}{8 d_m} \hat{A}_\perp^2 = \nu \frac{(\rho_m V_m)^2}{8 d_m} \hat{A}_\perp^2 \tag{5}$$

which expresses the output power with respect to the mass density of the oscillator ρ_m, the oscillator volume V_m, the acceleration amplitude $\hat{A}_\perp$, the parasitic mechanical damping coefficient d_m, the volume comprising the coil wire V_c, the coil filling factor k_c, the resistivity of the coil wire ρ_c, the flux density perpendicular to the oscillator displacement and the coil wire $B_\perp$ and the conversion effectiveness ν, respectively. The latter is a value between 0 and 1, where 1 means that maximum power is converted at the resonance frequency at a given excitation $\hat{A}_\perp$.

In literature, the proportionality of P_{avg} to $A_\perp^2$ is sometimes taken as reason to benchmark harvesters with respect to the power density divided by $A_\perp^2$. However, as Arnold already found, this approach does not correctly consider the impact of, e.g., the mechanical damping coefficient d_m and volume of the oscillator V_m [3]. In fact, the interdependencies and limitations result into a non-trivial impact of ambient conditions and boundary parameters on the parameters in Equation (5). To simplify the discussion, the parameters are handled independently and size is considered by a length scaling factor s.

Whereas the coil filling factor k_c, the flux density $B_\perp$, the resistivity ρ_c and the mass density ρ_m are independent of size and excitation, the coil volume V_c and the oscillator volume V_m are proportional to s^3. The role of the mechanical damping coefficient d_m depends on the dominating damping model. From the damping mechanisms in a harvester only laminar viscid damping, *i.e*.,

- viscid drag
- lateral laminar flow Couette damping
- lateral laminar flow Stokes damping (Stokes damping here refers to the expression for small frequencies and air gaps)
- perpendicular laminar flow squeeze film damping

each resulting in $d_m \propto s$ [9], is to be considered. The other damping types are either negligible or, in cases such as eddy current damping, turbulent drag, thermoelastic damping, material hysteresis damping and friction, can usually systematically be minimized below laminar viscid damping.

As research in the field of sensors shows, viscid damping at small scales even dominates at very low pressures [10–14]. What complicates the discussion is the fact that at large scale, large oscillator displacements and, if amorphous materials are used, material damping can be significant. The question under which conditions viscid or material damping is dominating has not been answered. Therefore, two benchmarking parameters should be introduced.

3.1. Viscid Damping

First, assume that laminar viscid damping dominates the system. With $d_m \propto s$ the conversion effectiveness depends on the harvester size. Let us say the effectiveness of a harvester with a volume of $1\,\mathrm{cm}^3$, namely $\nu(V = 1\,\mathrm{cm}^3)$, is known. If the harvester dimensions are related to the same volume, *i.e.*, $V_c(s) = s^3 V_c(V = 1\,\mathrm{cm}^3)$ and $d_m(s) = s d_m(V = 1\,\mathrm{cm}^3)$ the effectiveness would change as follows.

$$\nu(V) = \frac{1}{1 + \frac{\rho_c d_m}{V_c k_c B_\perp^2}} = \frac{1}{1 + \frac{1-\nu(V=1\,\mathrm{cm}^3)}{\nu(V=1\,\mathrm{cm}^3)} s^{-2}} \tag{6}$$

The relation is plotted in Figure 1a for different values $\nu(V = 1\,\mathrm{cm}^3)$ and indicates that the conversion effectiveness drops with $\nu \to s^2$ for harvesters at smaller dimensions and reaches unity for large s. Clearly, besides unity there is no physically defined benchmark or limit for $\nu(V = 1\,\mathrm{cm}^3)$ and a value needs to be taken from realized prototypes.

Figure 1. (**a**) conversion effectiveness ν with respect to scaling factor s according to Equation (6) and (**b**) average power P_{avg} at the eigenfrequency according to Equations (5) and (10) for different $\nu(V = 1\,\mathrm{cm}^3)$. Dashed lines denote slope of limits.

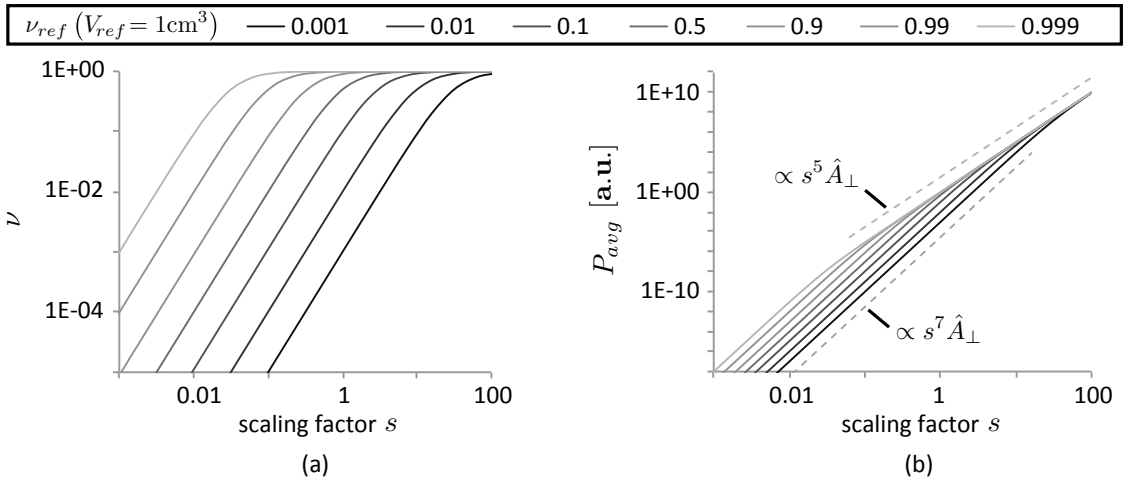

The corresponding output power of a harvester can be found with the help of Equation 5 and inserting the reference values including $m(s) = s^3 m(V = 1\,\mathrm{cm}^3)$. Figure 1b shows that for large s and respectively $\nu = 1$ the power is $P_{avg} \propto s^5 \hat{A}_\perp^2$. In contrast, for small s (and, of course, for unbeneficial designs) and $\nu \to s^2$ the power scales according to $P_{avg} \propto s^7 \hat{A}_\perp^2$. Both limits have already been identified by Arnold [3].

To relate the output power of a harvester to its particular volume, the length scaling factor can be replaced by $s^3 = V/\,\mathrm{cm}^3$ with the harvester volume V in cm^3 and the following BPs can be found. For large volumes there is

$$BP_{(V\to\infty)} = \frac{P_{avg}}{V^{\frac{5}{3}} \hat{A}_\perp^2} \cdot \frac{\mathrm{cm}^{\frac{5}{3}} (\mathrm{ms}^{-2})^2}{\mu\mathrm{W}} \tag{7}$$

and for small volumes

$$BP_{(V\to 0)} = \frac{P_{avg}}{V^{\frac{7}{3}} \hat{A}_\perp^2} \cdot \frac{\mathrm{cm}^{\frac{7}{3}} (\mathrm{ms}^{-2})^2}{\mu\mathrm{W}} \tag{8}$$

with P_{avg} in $\mu\mathrm{W}$, V in cm^3 and $A_\perp$ in ms^{-2}. Note: the respective units are used, because SI units are not common.

Interestingly, for the range of intermediate volumes one could apply the average normalization parameter

$$BP_{(V_{avg})} = \frac{P_{avg}}{V^2 \hat{A}_\perp^2} \cdot \frac{\mathrm{cm}^2 (\mathrm{ms}^{-2})^2}{\mu\mathrm{W}} \tag{9}$$

which directly results from Equation (5) for d_m and ν independent of s.

These three parameters have already been pointed out by Arnold [3]. A more complicated but more accurate and continuous BP can now be found by considering the scaling of the conversion effectiveness in detail. Inserting Equations (6) into (5) one gets

$$P_{avg} \propto \frac{1}{1 + \frac{1-\nu_{ref}}{\nu_{ref}} \cdot s^{-2}} s^5 \hat{A}_\perp^2 \tag{10}$$

With the reference values $\nu_{ref} = \nu\,(V_{ref})$ and $V_{ref} = 1\,\mathrm{cm}^3$ one can derive a global BP (c)

$$BP_{(c)} = P_{avg} \cdot \frac{1 + \frac{1-\nu_{ref}}{\nu_{ref}} \cdot \left(\frac{V}{V_{ref}}\right)^{-\frac{2}{3}}}{\left(\frac{V}{V_{ref}}\right)^{\frac{5}{3}} \hat{A}_\perp^2} \cdot \frac{(\mathrm{ms}^{-2})^2}{\mu\mathrm{W}} \tag{11}$$

which allows to compare harvesters based on the maximum normalized conversion effectiveness found or defined for a volume of $1\,\mathrm{cm}^3$. Consequently, based on a reference conversion effectiveness ν_{ref} harvesters can be compared only with the help of the single parameter BP (c) that considers the scaling discussed with Figure 1.

3.2. Material Damping

Having derived a BP for the assumption that viscid damping dominates the system, one can similarly find a parameter for the case that material damping is dominant. According to Appendix A, material damping is independent of the excitation acceleration but proportional to the frequency and

volume (compare Equations (22)–(24)). Therefore, based on the arbitrarily chosen reference value $\nu_{ref} = \nu(V_{ref} = 1\,\mathrm{cm}^3, \omega_{ref} = 2\pi 50\,\mathrm{Hz})$ the effectiveness is

$$\nu(V, \omega_0) = \frac{1}{1 + \frac{1-\nu_{ref}}{\nu_{ref}} \frac{\omega_0}{\omega_{ref}}} \tag{12}$$

and the output power is

$$P_{avg} \propto \frac{1}{1 + \frac{1-\nu_{ref}}{\nu_{ref}} \cdot \frac{\omega_0}{\omega_{ref}}} \cdot s^3 \frac{\omega_{ref}}{\omega_0} \hat{A}_\perp^2 \,. \tag{13}$$

The corresponding plots are shown in Figure 2. Consequently, the corresponding BP (d)

$$BP_{(d)} = P_{avg} \cdot \frac{1 + \frac{1-\nu_{ref}}{\nu_{ref}} \cdot \frac{\omega_0}{\omega_{ref}}}{\frac{V}{V_{ref}} \frac{\omega_{ref}}{\omega_0} \hat{A}_\perp^2} \cdot \frac{(\mathrm{ms}^{-2})^2}{\mu\mathrm{W}} \tag{14}$$

can be derived.

Figure 2. (**a**) conversion effectiveness ν with respect to scaling factor s according to Equation (12) and (**b**) average power P_{avg} at the eigenfrequency according to Equation (13) for different ν_{ref}.

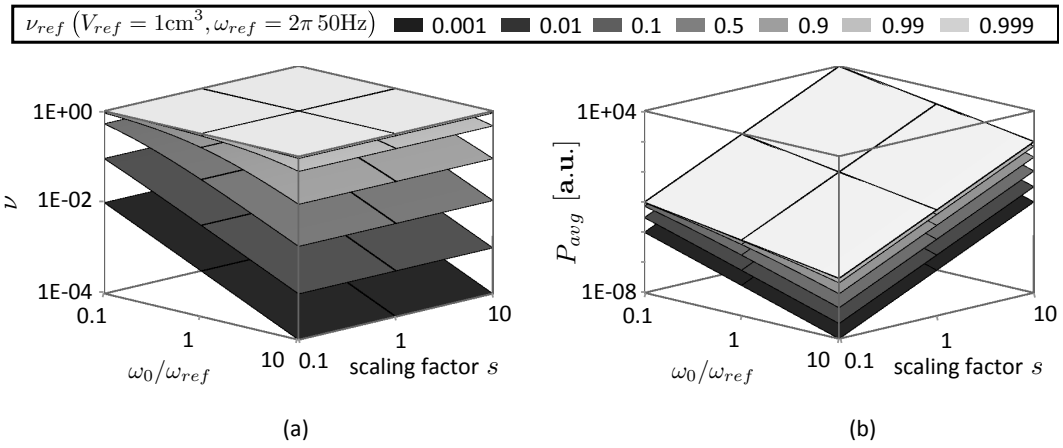

The two BPs (c) and (d) are quite different. Generally it is not clear under which conditions viscid damping or material damping is dominating, and the question of a fair benchmark parameter cannot be conclusively answered. On the one hand, one could claim that vacuum packaging of harvesters would allow to reduce viscid damping and generally apply BP (d). On the other hand, if harvesters are not used in vacuum and viscid damping is indeed dominating, the usage of BP (d) would treat harvesters with low ω_0 and large V preferentially; in other words, it would discriminate the other ones. Therefore, applying both parameters collectively to prototypes does not possibly allow to find an optimum design, but should help to identify promising designs.

Before applying the BPs to published prototypes some limitations should be kept in mind. Firstly, BP (c) and (d) both assume that any dimension of the harvester scales proportionally to the length scaling factor. However, according to [8] the oscillator amplitude is

- inversely proportional to ω_0 at a given acceleration
- proportional to the acceleration at a given ω_0 and

- proportional to s^2 when $d_m \propto s$ and constant when $d_m \propto s^3$

A fair comparison of a harvester design principle would therefore be based on excitation levels that result in a similar ratio of the penetrated to the total harvester volume. The volume that is not penetrated and would therefore not have been considered if a harvester had been designed for low accelerations could be subtracted from V.

Secondly, the aspect ratio of the harvester defines the design freedom and might on the one hand have an impact on the mechanical damping. Additionally, it influences the ratio of the penetrated to the harvester volume. Since it is not clear how both effects can be mathematically considered, one has to take BP values of harvesters with different aspect ratio with care.

Thirdly, the "total" harvester volume reported for harvester prototypes does not always include the same components. In some cases an electronic circuit or a large, more robust housing is considered. An effective total volume that includes a minimal closed housing but excludes the electronic circuit could serve as common base for discussion.

Finally, additional aspects and limitations such as a required lifetime, temperature or shock resistance or a maximum flux density in the surroundings of a harvester can reduce the design freedom and consequently the harvester power.

Not least for the lack of data all these aspects can hardly be considered. If benchmarking results, however, are carefully interpreted, BP (c) and (d) can serve as an appropriate basis for the comparison of resonant electrodynamic harvesters.

4. Benchmarking of Published Prototypes

Figure 3 contains the BPs (a)–(c) applied to the reviewed electrodynamic harvesters in [1]. As several prototypes feature a similar design but different performance, volume, *etc*., the harvesters are referenced by two numbers: "(?)" denotes the design number introduced in our review paper [1] and a single number "?" the benchmark value in the benchmark plots. Important values of these harvesters are collected in Tables 1 and 2. Note: The harvester volumes are the total volumes including the volume that was penetrated by the oscillator, the housing and possibly an electronic circuit. If the output power was only published after rectification, a factor of 1.3 was added.

The BP values in Figure 3 are proportional to the areas of the circles. If multiple measurements at different excitations have been published for a prototype, the diagrams contain the largest value with respect to the particular BP.

As discussed in the previous sections, a low performance value must not necessarily be due to a disadvantageous harvester design but could also result from

- measurements taken only at excitations where the BPs result in low values
- an unfavorable aspect ratio, housing or included electronic circuit
- restricting boundary conditions
- a non-resonant harvester concept with different physics and, finally
- the fact, that the harvester was not effectively optimized

Figure 3. Benchmark plots for electrodynamic harvesters. Plots show the maximum performance of each harvester according to the respective BP as well as available measurement data and with respect to the corresponding acceleration and frequency. Values are proportional to the area of circle and according to Table 1.

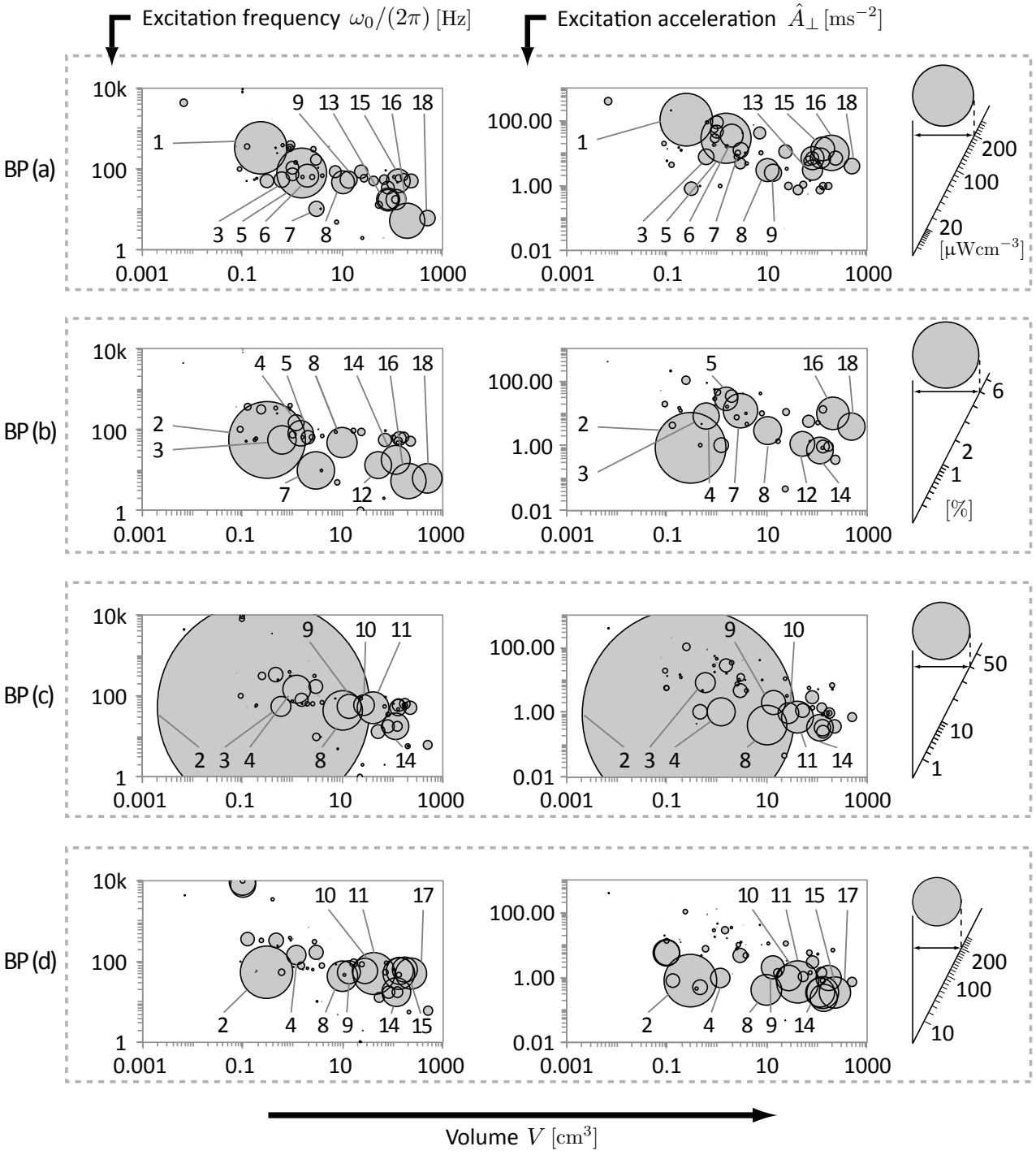

In many publications the geometry is not completely given and the harvester is not fully characterized. The lack of data complicates the interpretation of the results, making it impossible to identify a single beneficial design approach.

In all benchmark plots one recognizes the trend that smaller harvesters have been designed for higher frequencies. The reason is probably the difficulty to design harvesters with fragile springs of low stiffness. The decreasing oscillator amplitude at higher frequencies as well as smaller volumes additionally helps to prevent fatigue and to reduce the mechanical damping. As the discussion of the other BP (a) and (b) refers to BP (c) and (d), the comparison of published harvesters starts with the latter parameters.

Table 1. Harvester parameters corresponding to Figure 3 *estimated* / cited from published values. Multiple values are provided if maximum performance at different BPs is based on different measurements. If measured power was rectified, a compensation factor of 1.3 was added.

#	Reference	$V[\mathrm{cm}^3]$	$h[\mathrm{mm}]$	$\omega/2\pi[\mathrm{Hz}]$	$\hat{A}_\perp[\mathrm{ms}^{-2}]$	$P_{avg}[\mu\mathrm{W}_{\mathrm{avg}}]$
1	[15] MKI	0.24	*9*	322	102	530
2	[16] MKII	0.3	6.2	51.6	0.83	45
3	[17]	0.6	6	54	7.9	115
4	[18]	1.2	3	143	1	12
5	[19]	*1.50*	*15*	80	28	3000
6	[20]	*2.0*	*11*	66	34.4	830
7	[21]	*3.0*	*12*	10	11.8	545
8	[8] (updated)	10.0	36.5	45.3	3	4200
				44.6	0.4	138
9	[22]	*13.3*	*32*	55.9	2.0	2050
					2.5	3100
10	[23]	27	-	57	0.98	*1200*
11	[24] PMG7	41.3	-	50	0.71	3000
12	[25]	*52*	*40*	13.1	1.1	2000
13	[26,27]	80.0	-	17	7	*33*, *800*
					3	*26*, *000*
14	[28]	117	53	17.2	0.35	*2850*
15	[29]	130.7	55	50	13.9	*58*, *500*
16	[30]	*200*	*160*	5.4	10	200, 000
17	[31]	229	63	50	0.35	*2280*
18	[32]	500	100	6	0.71	15, 000

Table 2. Key parameters of selected harvesters in SI units *estimated*/simulated/ cited/computed* from published values. The column "Reference" denotes the particular publication, column "#" was introduced to refer to the corresponding benchmarking value in Figure 3 and the column "Design" refers to our review paper [1] to provide the design principle of the harvester. Note: the key parameters are according to measurement data that provide maximum performance according to BP (c) in Section 3. $B_\perp$ had to be adapted if wire was not perpendicular to direction of motion.

#	Design	Reference	V_c/V	k_c	$B_\perp$	$\frac{V_c k_c B_\perp^2}{V}$	d_m	ν	m/V	$\hat{X}_\perp/h$ [1]
1	harvester (1)	[15] MKI	*0.8%*	*0.50*	*0.15*	8.5×10^{-5}*	*0.027*	*0.04**	*2100*	*5%*
2	harvester (1)	[16] MKII[1]	0.7%*	0.67	*0.23*	2.4×10^{-4}*	0.00075*	*0.86**	2000*	*18%*
3	harvester (27)	[17]	-	-	-	-	*0.0001*	-	*81*	-
4	harvester (30)	[18]	7.7%	1.00	0.33	8.4×10^{-3}	*0.077*	*0.89*	2900	*0.8%*
5	harvester (8)	[19]	-	-	-	-	-	-	*1000*	*37%*
6	harvester (14)	[20]	-	-	-	-	-	-	-	-
7	harvester (10)	[21][2]	*0.5%*	*0.13*	*0.02*	3.7×10^{-6}*	-	*0.006**	*1100*	-
8	harvester (28)	[8]	4.5%	0.38	0.67	7.7×10^{-3}	0.18	0.96	3500	1.5%
9	similar to (23)	[22]	*2.6%*	0.60	*0.18*	5.05×10^{-4}	*0.085*	*0.82*	*1000*	*1.4%*
10		[23]	-	-	-	-	-	-	-	-
11		[24] PMG7	-	-	-	-	-	-	2050	-
12	harvester (1)	[25]	-	-	-	-	-	-	820	-
13		[26,27]	-	-	-	-	-	-	-	-
14		[28]	-	-	-	-	-	-	-	-
15	harvester (26)	[29]	-	-	-	-	-	-	-	-
16	harvester (5)	[30]	-	-	-	-	-	-	177	-
17		[31]	-	-	-	-	-	-	-	-
18	NOT equal to (7)	[32]	-	-	-	-	-	-	-	-

[1] $\hat{X}_\perp$ is maximum value appearing at high acceleration.

4.1. BP (c): Resonant Electrodynamic Harvesters with Viscid Damping

For BP (c) and Equation (10) a reference conversion effectiveness $\nu_{ref} = \nu\,(V_{ref} = 1\,\mathrm{cm}^3)$, $\nu_{ref} = 0.93$ is assumed. This value was reversely computed from Equation (6) for harvester number 2 [16] and is the largest reported reference effectiveness, followed by 8 with the normalized value $\nu\,(V_{ref} = 1\,\mathrm{cm}^3) = 0.84$. In fact, the estimated effectiveness of 4 with $\nu\,(V_{ref} = 1\,\mathrm{cm}^3) = 0.95$ slightly exceeds the value of harvester 2. However, the value was not taken because the damping could only be estimated.

As expected for viscidly damped harvesters, no correlation can be noted in the plot of BP (c) versus volume and the frequency of maximum power (which, for all resonant harvesters, is the eigenfrequency). The diagram versus volume and acceleration indicates that a higher performance can be realized at smaller acceleration. In fact, harvesters of low performance often seem to be deliberately measured at

high accelerations to reach a considerable absolute power level. Additionally, since which harvester was limited by which damping type is not reported, a dominating impact of material damping could be a second reason.

As already stated, the best performing harvester is number 2 [16]. Its design corresponds to the one labelled (1) in our review paper [1]. With a very low d_m the largest ν related to a volume of $1\,\mathrm{cm}^3$ and the largest $(m^2/d_m)/V^{5/3}$ were reached, although the harvester neither features the maximum m/V nor $V_c k_c B_\perp^2/V$. The performance could even be increased, because measurements have only been provided for a single excitation acceleration, which resulted in a large amplitude and penetrated volume. At a very small acceleration the total volume could be up to 35% smaller.

However, to interpret the high performance, two aspects have to be considered. Firstly, the harvester volume does not include a housing. Secondly and more important, this harvester is nonlinear due to a stiffening effect of the spring. Due to the stiffening, the output power increases when the harvester is measured at a frequency upsweep until it suddenly drops. The frequency of power break down is random and if the harvester is measured at a downsweep this point cannot be reached [16,33]. To our knowledge, by now the maximum upsweep power has not been reached at practical conditions.

The comparison of publications [16,34] provides even another confusing result. Both report measurements of exactly the same harvester at the same excitation but only 40% output power in [34]. The authors explained the higher performance by a better alignment of the beam in [16] that was supposed to reduce mechanical damping. Due to the lack of a mechanical characterization, this explanation has not been verified. (Damping was investigated by measuring the induced voltage which, due to a varying $B_\perp$, cannot provide reliable values. Consequently, the authors' observation of an increasing Q-factor for stronger acceleration was rather due to a decreasing electrodynamic coupling than a decreasing damping. The order of magnitude of the damping value in Table 2 that was derived from the published Q-factor, however, should be correct.)

In fact, even if the stiffening effect is not considered, the performance of number 2 is high, for which three reasons can be identified. Firstly, a low mechanical damping was realized due to a long clamped-free beryllium copper beam spring. Secondly, despite a small oscillator volume, the oscillator mass was increased by attaching a tungsten mass with a mass density of $16,000\,\mathrm{kg/m^3}$. Thirdly, the magnetic circuit consisted of multiple magnets combined with back iron to realize a comparably high flux density. The effective flux density was only reduced by the fact that the wire of the circular coil was not perpendicular to the direction of motion. Finally, considering that the harvester was not comprehensively optimized, it seems even possible to increase the output power.

A second well performing harvester with a volume more than an order of magnitude above is the cylindrical prototype 8 with design (28). Here, the maximum m/V and a good $V_c k_c B_\perp^2/V$ have been realized even with the housing included by compact packaging of membrane springs, coils, oscillator and housing and respectively an effective magnetic circuit design with nearly closed back iron.

However, compared with harvester 2 and the assumption $d_m \propto s$ the mechanical damping is a factor of 75 higher. The reason is a significant material damping due to high stress values in the springs. The large d_m strongly decreased $(m^2/d_m)/V^{5/3}$. Note: Due to the high $V_c k_c B_\perp^2/V$ the effectiveness still was $\nu = 0.96$ and respectively $\nu_{ref} = 0.84$ related to $1\,\mathrm{cm}^3$.

Other well performing harvesters are the commercial Perpetuum devices 14 and 15 [24,28] with a design probably according to [35–37]. Unfortunately, detailed data besides the output power is missing.

A very similar performance was also realized with the harvester 4 according to design (30). It features the largest $V_c k_c B_\perp^2/V$ and the second largest m/V. However, a comparably high damping reduced especially $(m^2/d_m)/V^{5/3}$.

All these harvesters contain a magnetic circuit with flux conducting components. In fact, two harvesters based on a simple magnet without flux guidance provided a good output power as well. The harvester 9 in [22] contained a magnet fixed to a CuSn6 membrane spring to vibrate towards a circular coil. Unfortunately, the harvester was not mechanically characterized. Based on the given oscillator mass as well as the tabled dimensions and drawings, m/V must have been approximately 1000. Estimating the mechanical damping coefficient from Equation (5) with subsequently simulated magnetic circuit results in $d_m \approx 0.085$ and a $\nu \approx 0.85$. This low damping coefficient allowed to compensate the low flux density.

The harvester 3 [17] with design (27) contained a very small magnet that was fixed to a silicon coil and penetrated a coil at vibration. Due to the magnetic circuit with a $V_c k_c B_\perp^2/V$ of about $10^{-5}..10^{-4}\,\mathrm{T}^2$ and a m/V of only $80\,{}^{\mathrm{kg}}/_{\mathrm{m}^3}$, the damping value must have been in the range of $d_m \approx 0.0001$, which would even be far below the value of harvester 2 at twice the volume. Provided that the measured values are correct, the key to the low damping was the wet etched silicon membrane spring with long beams.

Finally, it is worth mentioning the harvester in [38] according to design (13). Although it was fabricated by DRIE from bulk silicon for a minimum mechanical damping, the damping coefficient is large and the performance is low. As new results for a device with chemically polished sidewalls [39] have not been published, the damping value might be due to the rough surface after DRIE.

Since all these well performing harvesters have not been comprehensively optimized, the question whether a certain design is beneficial cannot be satisfiably answered. Nevertheless, beneficial design aspects can be identified and will be summarized in Section 5.

4.2. BP (d): Resonant Electrodynamic Harvesters with Material Damping

Benchmarking with BP (d) is based on a reference conversion effectiveness of $\nu_{ref} = (V_{ref} = 1\,\mathrm{cm}^3, \omega_{ref} = 2\pi 50\,\mathrm{Hz}) = 0.965$, which was the maximum value found and reached by 8.

Compared with BP (c), the plot of BP (d) suggests increasing performance values for lower accelerations and (less significant) higher frequencies. This observation corresponds to the assumption that stress and material damping are reduced at the lower oscillator amplitudes.

As for BP (c) also at BP (d) harvester 2 is the best performing prototype. The reasons are the same, low d_m, high m/V and a good $V_c k_c B_\perp^2/V$. According to these parameters, the oscillator amplitude at the measured acceleration must have been ca. $1\,\mathrm{mm}$, which is comparably large and, in fact, an indication for significant material damping. Consequently, measurements at a lower excitation could decrease d_m and result in an even better performance.

A very similar performance was reached by harvesters 11, 15, 8 and 14. Whereas the design of 11, 15 and 14 is not exactly known, the good performance of harvester 8 was due to maximum value of m/V and the second largest $V_c k_c B_\perp^2/V$. The mechanical damping was identified as material damping and

when compared with the damping value of harvester 2 was a factor of 9 larger (Note: The factor differs from what was found in the previous section, because damping scales differently).

Similar to what was explained for BP (d), as the harvesters have not been comprehensively optimized, the results only allow to identify beneficial design aspects, which are summarized in Section 5.

4.3. BP (a): Power Density

The power density BP (a) versus volume and acceleration does not show a clear correlation. However, a comparison with BP (c) indicates the tendency that, despite a comparably unbeneficial harvester design, simply a large harvester volume or strong acceleration can result in a high power density.

For example, prototype 1 [15] designed equal to (1) reached the maximum reported value of $2.2\,{}^{\mathrm{mW_{avg}}}/_{\mathrm{cm^3}}$. Since that prototype featured a comparably high damping, an acceleration of $\hat{A}_{\perp} = 102\,\mathrm{ms}^{-2}$ was necessary.

The non-resonant pendulum harvester 5 [19] (design (8)) provided similar $2\,{}^{\mathrm{mW_{avg}}}/_{\mathrm{cm^3}}$ at $\hat{A}_{\perp} = 28\,\mathrm{ms}^{-2}$ and 80 Hz in the state of continuous rotation.

For comparison, the energy of lithium ion or alkaline batteries with an energy density of approximately $400\,{}^{\mathrm{mWh}}/_{\mathrm{cm^3}}$ [40] can be harvested within less than 9 days (time span increases when rectifying and voltage control circuit are considered) when $BP_{(a)} = 2\,{}^{\mathrm{mW_{avg}}}/_{\mathrm{cm^3}}$. With harvesters showing a high performance according to BP (c), the cited power density values are already possible at lower accelerations and respectively smaller volume. Moreover, higher values are possible if the following correlation is considered: The output power is limited by the squared total change of flux and the squared oscillation frequency.

4.4. BP (b): Vibration Power Limit

BP (b) requires the assumption of a mass density value. Since BP (b) is supposed to be a physical limit, the highest mass density of an element of the periodic table, the density of Osmium with $\rho_m = 22.6\,{}^{\mathrm{g}}/_{\mathrm{cm^{-3}}}$, is taken. If compared with BP (c), the plots of BP (b) versus volume and frequency and respectively volume and acceleration show a trend of higher performance towards larger volumes, higher accelerations and lower frequencies.

The maximum value of 3% according to BP (b) is reached by harvester 2 [16] with the design (1). Here, the oscillator displacement amplitude approaches the theoretical optimum of $\hat{X}_{\perp}/h = 0.25$. Additionally, due to the small mechanical damping and an additional tungsten mass increasing the effective mass density of the oscillator, the necessary acceleration is low.

A performance of 0.7% was realized by harvester 7 [21] with design (10), and is due to the high excitation acceleration and the low frequency that allows to approach high displacement amplitudes (values have not been reported).

The performance of 0.43% of harvester 16 [30] (design (5)) results from its even larger volume, lower frequency and a similar strong acceleration.

The fourth best result of 0.42% is provided by 8, although its frequency is comparably high and the acceleration (measurement at $3\,\mathrm{ms}^{-2}$) comparably low. The reason, similar as mentioned in the discussion of BP (a), is its good performance according to BP (c).

The performance values realized according to BP (b) are small, because neither was the mass density of Osmium used, nor the power loss due to the mechanical damping and the coil resistance (which account for more than 50%) could be avoided. Comparing the values with BP (c) and (d), however, shows that BP (b) often is a good indicator for a well designed resonant electrodynamic harvester.

5. Implications on Design

The question which harvester design should be preferred is discussed based on the high performing harvesters according to BP (c) and (d). The best performing harvesters at BP (d) are also performing well at BP (c), and vice versa. This aspect shows that these designs stand out from the other published harvesters and feature beneficial design aspects.

A high $V_c k_c B_\perp^2/V$ can be realized with the help of magnetic circuit designs effectively guiding the flux. In combination with these magnetic circuits solenoidal coils have been found optimal.

High values of m/V were realized by a compact (especially cylindrical) design or a supplementary mass with high mass density. The latter increases the effective mass density of the oscillator such that the oscillator volume can be decreased for a smaller viscid damping. Due to its large volume, the magnetic circuit was usually used as oscillator. For example, for harvester 2, the ratio of the coil to magnetic circuit volume is approximately 20% and for 8 approximately 7%. In fact, the risk of eddy currents and an impact of surrounding parts on the harvester behavior is reduced when the coil is used as oscillator.

As long as the oscillator amplitude is small compared with the dimensions of the harvester, a low d_m can compensate for low values of $V_c k_c B_\perp^2/V$ and m/V. Detailed studies of the mechanical damping have not been found in literature, and the impact and suitability of different designs cannot be compared. The comparison of the harvester designs suggests that the dominant damping phenomena are material damping, in special cases friction [41] and possibly laminar viscid damping.

Low damping was provided by a single fixed-free beam [16,34]. Due to the low fatigue strength of silicon, the beam was out of an amorphous material. It is not clear whether material, viscid or even another damping type was dominating. As the authors reported, the quality factor of the oscillation strongly depended on the accuracy of the clamping of the beam. Our own investigations suggested that the critical point is to avoid momentums from an angle between the beam axis and the fixation line as well as an excentrical mass. A solution is the usage of stress compensated approaches [10,42,43].

Another opportunity is membrane springs, because the closed boundary can reduce the impact of the clamping. Spring designs with long meandered or spiral beams can effectively distribute the stress that appears at the oscillator deflection. However, as our own measurements with harvester 8 suggested, membrane springs need to be designed carefully to prevent high stress from nonlinear geometrical effects. Additionally, for the spring design one has to consider the trade-off between long beams providing low stress and a high stiffness ratio that ensures a defined oscillation at perpendicular forces.

Lowest damping was possibly realized with a single crystalline silicon membrane spring of comparably long beams [17]. However, also amorphous materials may provide low damping (compare the harvesters with beryllium copper, silicon and steel 304 beam in [16] and the CuSn6 membrane spring in [22], the latter under consideration of the short beams). Due to the lack of data a detailed analysis of the materials is still necessary.

Finally, as the example of the beam harvester 3 [16] shows, low damping values can possibly even at fair excitation levels result in an oscillator amplitude that reaches its geometrical or fatigue limit. The answer to that problem: It is not a bug, it is a feature! Such a low damping could be used either to reduce the oscillator mass or to increase the harvester volume to harvest more power. Alternatively, for a certain range of excitations one could limit the oscillator amplitude by decreasing the load resistance down to $R_l = R_c$, which increases the harvester power due to an increased electrical damping. For excitations beyond, spring-like end stops seem to be a promising solution (compare design (18)). On the one hand, the oscillator velocity at zero crossing and consequently the power are increased. On the other hand a wideband plateau of maximum power is realized. Right now, however, the challenge is rather to identify possibilities to reduce the damping and not the oscillator amplitude.

Therefore, to maximize the performance of electrodynamic harvesters, the harvesters should systematically be optimized under consideration of the mechanical damping phenomena.

6. Conclusions

The benchmarking parameters can serve as starting point to evaluate harvesters and to identify a good harvester design. Indeed, a completely fair benchmarking is practically not possible. First, the complex impact of all ambient and boundary conditions cannot be comprehensively considered. Second, the various different requirements on harvesters cannot be all quantified. Third, important data of prototypes, which are needed for benchmarking, are often not published. Due to the complex impact of the boundary conditions and different practical requirements that possibly limit the design freedom, multiple benchmarking parameters are necessary. Consequently, there cannot be *the* best design approach. Detailed data of a harvester, such as the oscillator mass and volume, the coil wire volume and resistivity, the flux density and the mechanical damping, all related to the total volume and the excitation acceleration and frequency, have to be considered to truly evaluate the capabilities of a harvester design.

The novel benchmarking parameters BP (c) and (d), which were introduced in this paper, can nevertheless serve as a starting point for benchmarking. They allow to compare resonant-type electrodynamic harvesters based on the practical impact of the most important parameters: the excitation and the harvester volume. For the first time they consider the important dependencies of the mechanical damping and the conversion effectiveness.

A. Derivation of Material Damping

The dependency of the material damping on the dimensions and excitation should be explained with the help of a single membrane spring, which can be modeled as a setup of multiple fixed-guided Bernoulli beams assuming pure bending stress. For the given oscillator mass and eigenfrequency, the total spring stiffness k for a membrane spring containing j beams is defined by

$$k = j\frac{Ebh^3}{l^3} \tag{15}$$

with E being the Young's modulus, b the width, h the height and l the length of a single beam. According to [44] the material damping coefficient is proportional to the damping energy per cycle

$$d_{m_h} = \frac{J\left(\frac{\hat{\sigma}}{\sigma_L}\right)^n \alpha j V_{beam}}{\pi \omega_0 \hat{X}_\perp^2} \tag{16}$$

where V_{beam} is the total volume of a single beam, and J, n as well as σ_L are the specific material parameters with $2 < n < 3$ at peak stress levels in the material $\hat{\sigma} < \sigma_L$ [44]. The eigenform of a resonating tip loaded beam with a tip mass much larger than the mass of the beam equals the static bending line and a linear bending moment can be assumed. For that case Goodman [44] provided the geometry factor $\alpha = (n+1)^{-2}$, which was in slightly different form originally derived by Lazan in [45].

For a linear bending moment, the bending stress at the root of the fixed-guided beams depends on the deflection $\hat{X}_\perp$

$$\hat{\sigma} = \hat{X}_\perp \frac{3Eh}{l^2}, \tag{17}$$

whereas the deflection at the eigenfrequency is according to

$$\hat{X}_\perp = \frac{\omega_0 m}{d_{m_h} + d_e} \cdot \frac{\hat{A}_\perp}{\omega_0^2} = \frac{m\hat{A}_\perp}{\omega_0 d_{m_h} \frac{2}{2-\nu}} \tag{18}$$

and m is the relevant tip mass. Solving Equations (16) and (18) for d_{m_h} and equating gives

$$\hat{X}_\perp = \frac{ijV_{beam}\alpha J\left(\frac{\sigma}{\sigma_L}\right)^n}{\frac{\pi}{2}(2-\nu)\, m\hat{A}_\perp} \tag{19}$$

Note: this equation might be confusing as the oscillator displacement $X_\perp$ increases with the damping energy. The correct interpretation is that a higher damping energy can only be realized at a higher oscillator displacement. The following equations clarify that. By inserting into Equations (17) and (16) one can find

$$\begin{aligned} \hat{\sigma} &= \left(\frac{\frac{\pi}{2}(2-\nu)\, m\hat{A}_\perp}{ijV_{beam}\alpha J\sigma_L^{-n}} \cdot \frac{l^2}{3Eh}\right)^{\frac{1}{n-1}} \\ &= \left(\frac{\frac{\pi}{6}(2-\nu)\, m\hat{A}_\perp}{\alpha J\sigma_L^{-n}E} \cdot \frac{l}{ijbh^2}\right)^{\frac{1}{n-1}} \end{aligned} \tag{20}$$

and

$$\begin{aligned} d_{m_h} &= \frac{\left(\frac{\pi}{2}(2-\nu)\, m\hat{A}_\perp\right)^2}{\pi\omega_0\, ijV_{beam}\alpha J\left(\frac{\sigma}{\sigma_L}\right)^n} \\ &= \frac{\pi}{4\,\omega_0}\left(\frac{((2-\nu)\, mA_\perp)^{n-2}\, ijbh^{n+1}\alpha J E^n}{l^{2n-1}\sigma_L^n}\right)^{\frac{1}{n-1}} \end{aligned} \tag{21}$$

Now, whereas $A_\perp$ has no impact on other parameters, it is important to remember that a changing ω requires to adapt the spring stiffness k, which is according to Equation (15). Assume that the dimensions

generally correlate with the harvester dimensions but the spring height is adapted to provide the correct spring stiffness. Since advantageous amorphous materials with low damping have nearly $n = 2$ [44], the following correlations can be found.

$$d_m\left(\frac{A_\perp}{A_{\perp ref}}\right) \propto 1 \tag{22}$$

$$d_m\left(\frac{\omega_0}{\omega_{ref}}\right) \propto \left(\frac{\omega_0}{\omega_{ref}}\right) \tag{23}$$

$$d_m(s) \propto s^3 \tag{24}$$

Acknowledgements

The authors would like to thank the DFG for funding the graduate school 1322, Micro Energy Harvesting. Additionally, the first author thanks the Foundation of German Business (sdw) for his Ph.D. scholarship.

Conflict of Interest

The authors declare no conflict of interest.

References

1. Cepnik, C.; Lausecker, R.; Wallrabe, U. Review on electrodynamic energy harvesters-a classification approach. *Micromachines*, in press.
2. Mitcheson, P.D.; Yeatman, E.M.; Rao, G.K.; Holmes, A.S.; Green, T.C. Energy harvesting from human and machine motion for wireless electronic devices. *Proc. IEEE* **2008**, *96*, 1457–1486.
3. Arnold, D. Review of microscale magnetic power generation. *Magn. IEEE Trans.* **2007**, *43*, 3940–3951.
4. Stephen, N. On energy harvesting from ambient vibration. *J. Sound Vib.* **2006**, *293*, 409–425.
5. Mitcheson, P.D.; Green, T.C.; Yeatman, E.M.; Holmes, A.S. Architectures for vibration-driven micropower generators. *J. Microelectromechan. Syst.* **2004**, *13*, 429–440.
6. Mitcheson, P.; Reilly, E.; Toh, T.; Wright, P.; Yeatman, E. Performance limits of the three MEMS inertial energy generator transduction types. *J. Micromech. Microeng.* **2007**, *17*, 211–216.
7. Cepnik, C.; Wallrabe, U. On the Comparison, Scaling and Benchmarking of Electromagnetic Vibration Harvesters. In Proceedings of PowerMEMS 2011, Seoul, Korea, 15–18 November 2011; pp. 70–73.
8. Cepnik, C.; Radler, O.; Rosenbaum, S.; Ströhla, T.; Wallrabe, U. Effective optimization of electromagnetic energy harvesters through direct computation of the electromagnetic coupling. *Sens. Actuators A* **2011**, *167*, 416–421.
9. Hang Bao, M. *Micro Mechanical Transducers*; Elsevier Science: Amsterdam, The Netherlands, 2000; Volume 8.
10. Buser, R.; de Rooij, N. Very high Q-factor resonators in monocrystalline silicon. *Sens. Actuators A* **1990**, *21*, 323–327.

11. Johari, H.; Shah, J.; Ayazi, F. High Frequency XYZ-axis Single-Disk Silicon Gyroscope. In Proceedings of the IEEE 21st International Conference on Micro Electro Mechanical Systems, Tucson, AZ, USA, 13–17 January 2008; pp. 856–859.
12. Kim, B.; Hopcroft, M.; Candler, R.; Jha, C.; Agarwal, M.; Melamud, R.; Chandorkar, S.; Yama, G.; Kenny, T. Temperature dependence of quality factor in MEMS resonators. *J. Microelectromechan. Syst.* **2008**, *17*, 755–766.
13. Lifshitz, R.; Roukes, M. Thermoelastic damping in micro-and nanomechanical systems. *Phys. Rev. B* **2000**, *61*, 5600–5609.
14. Prikhodko, I.; Zotov, S.; Trusov, A.; Shke, A. Sub-degree-per-hour Silicon MEMS Rate Sensor with 1 Million Q-Factor. In Proceedings of the Transducers'11, IEEE, Beijing, China, 5–9 June 2011; pp. 2809–2812.
15. El-Hami, M.; Glynne-Jones, P.; White, N.; Hill, M.; Beeby, S.; James, E.; Brown, A.; Ross, J. Design and fabrication of a new vibration-based electromechanical power generator. *Sens. Actuators A* **2001**, *92*, 335–342.
16. Beeby, S.; Torah, R.; Tudor, M.; Glynne-Jones, P.; O'Donnell, T.; Saha, C.; Roy, S. A micro electromagnetic generator for vibration energy harvesting. *J. Micromech. Microeng.* **2007**, *17*, 1257–1265.
17. Park, J.; Bang, D.; Park, J. Micro-fabricated electromagnetic power generator to scavenge low ambient vibration. *Magn. IEEE Trans.* **2010**, *46*, 1937–1942.
18. Cepnik, C.; Wallrabe, U. A Flat High Performance Micro Energy Harvester Based on a Serpentine Coil with a Single Winding. In Proceedings of the Transducers'11, IEEE, Beijing, China, 5–9 June 2011; pp. 661–664.
19. Spreemann, D.; Manoli, Y.; Folkmer, B.; Mintenbeck, D. Non-resonant vibration conversation. *J. Micromech. Microeng.* **2006**, *16*, 169–173.
20. Ching, N.N.H.; Wong, H.Y.; Li, W.J.; Leong, P.H.W.; Wen, Z. A laser-micromachined multi-modal resonating power transducer for wireless sensing systems. *Sens. Actuators A* **2002**, *97-98*, 685–690.
21. Zorlu, O.; Topal, E.; Kulah, H. A vibration-based electromagnetic energy harvester using mechanical frequency up-conversion method. *Sens. J. IEEE* **2011**, *11*, 481–488.
22. Spreemann, D.; Manoli, Y. Electromagnetic Vibration Energy Harvesting Devices: Architectures, Design, Modeling and Optimization. PhD Thesis, University of Freiburg, Freiburg, Germany, 2012.
23. Waters, R.; Chisum, B.; Jazo, H.; Fralick, M. Development of an Electro-Magnetic Transducer for Energy Harvesting of Kinetic Energy and Its' Applicability to a MEMS-Scale Device. In Proceedings of the Nanopower Forum, Irvine, CA, USA, 2–4 June 2008.
24. Beeby, S.; Tudor, M.; Torah, R.; Roberts, S.; O'Donnell, T.; Roy, S. Experimental comparison of macro and micro scale electromagnetic vibration powered generators. *Microsyst. Technol.* **2007**, *13*, 1647–1653.
25. Saha, C.; O'Donnell, T.; Loder, H.; Beeby, S.; Tudor, J. Optimization of an electromagnetic energy harvesting device. *IEEE Trans. Magn.* **2006**, *42*, 3509–3511.

26. Hadas, Z.; Zouhar, J.; Singule, V.; Ondrusek, C. Design of Energy Harvesting Generator Base on Rapid Prototyping Parts. In Proceedings of the 13th Power Electronics and Motion Control Conference (EPE/PEMC), IEEE, Poznan, Poland, 1–3 September 2008; pp. 1665–1669.
27. Hadas, Z.; Singule, V.; Ondrusek, Č. Optimal design of vibration power generator for low frequency. *Solid State Phenom.* **2009**, *147*, 426–431.
28. *PMG27*. Technical report, Perpetuum Ltd.: Southampton, UK, 2009.
29. *PMG17*. Technical report, Perpetuum Ltd.: Southampton, UK, 2009.
30. Mann, B.; Owens, B. Investigations of a nonlinear energy harvester with a bistable potential well. *J. Sound d Vib.* **2010**, *329*, 1215–1226.
31. *PMG FSH*. Technical report, Perpetuum Ltd.: Southampton, UK, 2009.
32. Sasaki, K.; Osaki, Y.; Okazaki, J.; Hosaka, H.; Itao, K. Vibration-based automatic power-generation system. *Microsyst. Technol.* **2005**, *11*, 965–969.
33. Barton, D.; Burrow, S.; Clare, L. Energy harvesting from vibrations with a nonlinear oscillator. *J. Vib. Acoust.* **2010**, *132*, doi:10.1115/1.4000809.
34. Torah, R.; Beeby, S.; Tudor, M.; O'Donnell, T.; Roy, S. Development of a Cantilever Beam Generator Employing Vibration Energy Harvesting. In Proceedings of the PowerMEMS 2006, Berkeley, CA, USA, 29 November–1 December 2006; pp. 181–184.
35. Roberts (Hampshire, GB), S.; Perpetuum Ltd.. Electromechanical Generator for Converting Mechanical Vibrational Energy into Electrical Energy. Patent WO2007020383A1, 2007.
36. Roberts (Hampshire, GB), S.; Perpetuum Ltd.. Electromechanical Generator for Converting Mechanical Vibrational Energy into Electrical Energy. Patent WO2008132423A1, 2008.
37. Roberts (Hampshire, GB), S.; Perpetuum Ltd.. Electromechanical Generator for Converting Mechanical Vibrational Energy into Electrical Energy. Patent WO2009068856A3, 2009.
38. Kulkarni, S.; Koukharenko, E.; Torah, R.; Tudor, J.; Beeby, S.; O'Donnell, T.; Roy, S. Design, fabrication and test of integrated micro-scale vibration-based electromagnetic generator. *Sens. Actuators A* **2008**, *145*, 336–342.
39. Koukharenko, E.; Tudor, M.; Beeby, S. Performance improvement of a vibration-powered electromagnetic generator by reduced silicon surface roughness. *Mater. Lett.* **2008**, *62*, 651–654.
40. Friedrich, K.; Wagner, N.; Bessler, W. *Entwicklungsperspektiven von Li-Schwefel und Li-Luft-Batterien.* Technical report, Institut für Technische Thermodynamik, Deutsches Zentrum für Luft- und Raumfahrt e.V., Energiespeichersymposium Stuttgart 2012, Stuttgart, Germany, 3 September 2013.
41. Hadas, Z.; Ondrsek, C.; Singule, V. Power sensitivity of vibration energy harvester. *Microsyst. Technol.* **2010**, *16*, 691–702.
42. Stemme, G. Resonant silicon sensors. *J. Micromech. Microeng.* **1991**, *1*, 113–125.
43. Koyama, T.; Bindel, D.; He, W.; Quévy, E.; Govindjee, S.; Demmel, J.; Howe, R. Simulation Tools for Damping in High Frequency Resonators. In Proceedings of the IEEE Sensors, Irvine, CA, USA, 30 October–3 November 2005; pp. 1–4.
44. Goodman, L. Material damping and slip damping. In *Harris' Shock and Vibration Handbook*, 5th ed.; McGRAW-Hill: New York, NY, USA, 2002; pp. 36.1–36.30

45. Lazan, B. *Effect of damping constants and stress distribution on the resonance response of members.* Technical report, DTIC Document, 1952.